

On the detectability of H I 21-cm in Mg II absorption systems

S. J. Curran*

School of Physics, University of New South Wales, Sydney NSW 2052, Australia

Accepted —. Received —; in original form —

ABSTRACT

We investigate the effect of two important, but oft neglected, factors which can affect the detectability of H I 21-cm absorption in Mg II absorption systems: The effect of line-of-sight geometry on the coverage of the background radio flux and any possible correlation between the 21-cm line strength and the rest frame equivalent width of the Mg II 2796 Å line, as is seen in the case of damped Lyman- α absorption systems (DLAs). Regarding the former, while the observed detection rate at small angular diameter distance ratios ($DA_{\text{abs}}/DA_{\text{QSO}} > 0.8$) is a near certainty ($P > 0.9$), for an unbiased sample, where either a detection or a non-detection are equally likely, at $DA_{\text{abs}}/DA_{\text{QSO}} \geq 0.8$ the observed detection rate has only a probability of $P \lesssim 10^{-15}$ of occurring by chance. This $\gtrsim 8\sigma$ significance suggests that the mix of $DA_{\text{abs}}/DA_{\text{QSO}}$ values at $z_{\text{abs}} \lesssim 1$ is correlated with the mix of detections and non-detections at low redshift, while the exclusively high values of the ratio ($DA_{\text{abs}}/DA_{\text{QSO}} \sim 1$) at $z_{\text{abs}} \gtrsim 1$ contribute to the low detection rates at high redshift.

In DLAs, the correlation between the 21-cm line strength ($\int \tau dv/N_{\text{HI}}$) and the Mg II equivalent width ($W_r^{\lambda 2796}$) is dominated by the velocity spread of the 21-cm line. This has recently been shown not to hold for Mg II systems in general. However, we do find the significance of the correlation to increase when the Mg II absorbers with Mg I 2852 Å equivalent widths of $W_r^{\lambda 2852} > 0.5$ Å are added to the DLA sample. This turns out to be a sub-set of the parameter space where Mg II absorbers and DLAs overlap and the fraction of Mg II absorbers known to be DLAs rises to 50% (Rao et al. 2006). We therefore suggest that the width of the 21-cm line is correlated with $W_r^{\lambda 2796}$ for all systems likely to be DLAs and note a correlation between $W_r^{\lambda 2852}$ (Mg I) and N_{HI} , which is not apparent for the singly ionised lines. Furthermore, the 21-cm detection rate at $DA_{\text{abs}}/DA_{\text{QSO}} < 0.8$ rises to $\gtrsim 90\%$ for absorbers with $W_r^{\lambda 2852} > 0.5$ Å and large values of $DA_{\text{abs}}/DA_{\text{QSO}}$ may explain why the absorbers which have similar values of $W_r^{\lambda 2796}$ to the detections remain undetected. We do, however, also find the neutral hydrogen column densities of the non-detections to be significantly lower than those of the detections, which could also contribute to their weak absorption. Applying the $\int \tau dv/N_{\text{HI}} - W_r^{\lambda 2796}$ correlation to yield column densities for the Mg II absorbers in which this is unmeasured, we find no evidence of a cosmological evolution in the neutral hydrogen column density in the absorbers searched for in 21-cm.

Key words: quasars: absorption lines – cosmology: observations – galaxies: high redshift – galaxies: ISM – radio lines: galaxies

1 INTRODUCTION

Redshifted radio absorption lines can provide an excellent probe of the contents and nature of the early Universe, through surveys which are not subject to the same flux and magnitude limitations suffered by optical studies. In particular, with the H I 21-cm line we can probe the evolution of large-scale structure, as well as measuring any putative variations in the values of the fundamental constants at large look-back times, to at least an order of magnitude

the sensitivity provided by the best optical data. (Curran et al. 2004 and references therein).

However redshifted H I 21-cm absorbers are currently rare, with only 40 “associated” systems being detected in the hosts of radio galaxies and quasars (see table 1 of Curran et al. 2008) and another 40 “intervening” systems, which lie along the sight-lines to distant Quasi-Stellar Objects (QSOs), Table 1. In both cases, 21-cm absorption is predominantly detected at redshifts of $z \lesssim 1$, which for the associated systems could be due to the excitation/ionisation caused by the proximity to the active nucleus, where optical surveys tend to select the most UV luminous sources at high redshift (Curran et al. 2008).

* E-mail: sjc@phys.unsw.edu.au

Table 1. Searches for intervening redshifted H I 21-cm absorption systems. The redshift range (z_{abs}) is given as well as the number of detections and non-detections (n_{det} and n_{non} , respectively).

Reference	Type	z_{abs}	n_{det}	n_{non}
Brown & Roberts (1973)	DLA	0.69	1	0
Roberts et al. (1976)	DLA	0.52	1	0
Wolfe & Davis (1979)	DLA	1.78	1	0
Wolfe et al. (1981)	DLA	1.94	1	0
Brown & Mitchell (1983)*	sub-DLA	0.44	1	0
Briggs & Wolfe (1983)	Mg II	0.37–1.94	1	16
Wolfe et al. (1985)	DLA	2.04	1	0
Carilli et al. (1993)	Lens	0.69	1	0
Carilli et al. (1996)	DLA	2.77–3.20	0	3
de Bruyn et al. (1996)	DLA	3.39	1	0
Lovell et al. (1996)	Lens	0.19	1	0
Lane et al. (1998)	DLA	0.22–0.31	2	0
Chengalur et al. (1999)	Lens	0.89	1	0
Pihlström et al. (1999)	DLA	0.63	0	1
Chengalur & Kanekar (2000)*	DLA	0.28–0.48	0	2
Lane (2000)*	Mg II	0.21–0.96	1	55
Lane et al. (2000)	Ca II	0.09	1	0
Lane & Briggs (2001)*	Mg II	0.44	1	0
Kanekar & Chengalur (2001)	DLA	0.25–0.56	2	1
Kanekar et al. (2001)	Mg II	0.10	0	1
Kanekar & Chengalur (2003)	DLA	0.42–3.18	1	9
Kanekar & Briggs (2003)	Lens	0.76	1	0
Darling et al. (2004)	—	0.78	1	—
Kanekar et al. (2006)	DLA	2.35	1	0
Curran et al. (2007a)	Lens	0.96	1	—
Curran et al. (2007c)	DLA	0.66–2.71	1	2
York et al. (2007)	DLA	2.29	1	—
Gupta et al. (2009)	Mg II	1.10–1.45	9	26
Kanekar et al. (2009b)*	Mg II	0.58–1.70	4	35
Zwaan et al. (in prep.)	Mg II	~ 0.6	2	—

*Other detections reported, but which also appear in previous papers.

For the intervening systems, many arise in known damped Lyman- α absorption systems, which, at redshifts of $z_{\text{abs}} \gtrsim 1.7$, have the Lyman- α line shifted into the optical band, allowing direct measurements of the neutral hydrogen column densities ($N_{\text{HI}} \geq 2 \times 10^{20} \text{ cm}^{-2}$, by definition). Non-detections can be thereby attributed to high spin temperatures (Kanekar & Chengalur 2003) and/or poor coverage of the background flux (Curran et al. 2005) in the high redshift systems (see Equ. 1, Sect. 2.1).

Note, however, of the DLAs, the vast majority detected in 21-cm are also known Mg II absorbers, these traditionally being considered good candidates for the detection of 21-cm absorption at $z_{\text{abs}} \lesssim 1.7$, where the Lyman- α band is attenuated by the atmosphere. Two recent surveys of Mg II systems (at $1.10 < z_{\text{abs}} < 1.45$, Gupta et al. 2009 and $0.58 < z_{\text{abs}} < 1.70$, Kanekar et al. 2009b), have found a total of 13 new 21-cm absorbers between them, significantly increasing the number known at $z_{\text{abs}} \approx 1$ (Table 1). In these works, various parameters (related to the equivalent widths of the singly ionised and neutral metal lines) are discussed, although the effects of geometry are generally ignored: Curran & Webb (2006) attribute the high 21-cm detection rate in DLAs identified through Mg II, cf. Lyman- α , absorption to the fact that the Mg II transition traces a lower redshift range ($0.2 \lesssim z_{\text{abs}} \lesssim 2.2$, with ground-based telescopes, cf. $z_{\text{abs}} \gtrsim 1.7$). At redshifts of $z_{\text{abs}} \gtrsim 1.6$, the geometry of our flat expanding Universe, ensures that foreground absorbers are *always* at larger angular diameter distances than the background QSOs, meaning that their effective cov-

erage of the background radio continuum is generally reduced compared to the $z_{\text{abs}} \lesssim 1.6$ absorbers (particularly those at $z_{\text{abs}} \lesssim 1.0$). In this paper, we address this issue, investigating possible geometry effects on the Mg II sample as a whole, as well as discussing other possible effects on the detectability of 21-cm absorption.

2 FACTORS AFFECTING THE DETECTION OF 21-CM

2.1 General

The detectability of 21-cm absorption in a system lying along the sight-line to a radio source is determined from the total neutral hydrogen column density, N_{HI} , via

$$N_{\text{HI}} = 1.823 \times 10^{18} T_{\text{spin}} \int \tau dv, \quad (1)$$

where T_{s} [K] is the mean harmonic spin temperature of the gas and $\int \tau dv$ [km s^{-1}] is the velocity integrated optical depth of the line. The optical depth is defined via $\tau \equiv -\ln(1 - \frac{\sigma}{fS})$, where σ is the depth of the line (or r.m.s. noise in the case of a non-detection) and S and f the flux density and covering factor of the background continuum source, respectively. Therefore in the optically thin regime ($\sigma \ll fS$), Equ. 1 reduces to $N_{\text{HI}} = 1.823 \times 10^{18} \frac{T_{\text{spin}}}{f} \int \frac{\sigma}{S} dv$, and so with a measurement of N_{HI} (from the Lyman- α line), the velocity integrated “optical depth”, $\int \frac{\sigma}{S} dv$, gives the ratio of the spin temperature to the covering factor, T_{spin}/f .

The importance of each of these terms to the T_{spin}/f degeneracy is the subject of much debate, i.e. whether the large number of non-detections at high redshift are predominately due to high spin temperatures (Kanekar & Chengalur 2003), or whether the coverage of the background emission region also plays a rôle (Curran et al. 2005). For the majority of the Mg II systems, which have not been observed in the Lyman- α line, the situation is further complicated by the fact that the total neutral hydrogen column density is unknown, giving a threefold degeneracy from the integrated line strength. Therefore determining the relative spin temperature and covering factor contributions is currently impossible, although we can investigate possible geometry effects, which are independent of the assumptions used to determine these three unknowns while having a direct bearing on the covering factor.

2.2 Geometry effects

As stated above, Curran & Webb (2006) suggested that for DLAs (then 17 detections and 18 non-detections), the 21-cm detection rate could be influenced by geometry effects, where at redshifts of $z_{\text{abs}} \lesssim 1$ a foreground absorber can have a mix of angular diameter distance ratios, $DA_{\text{abs}}/DA_{\text{QSO}}$, depending upon the relative absorber and QSO redshifts, whereas at $z_{\text{abs}} \gtrsim 1$ the diameter distance ratio is *always* large ($DA_{\text{abs}}/DA_{\text{QSO}} \approx 1$). This is illustrated in Fig. 1 (top), where we show the $DA_{\text{abs}}/DA_{\text{QSO}}$ distribution for the whole Mg II absorber sample: While the histogram for the line strengths appears to have a Gaussian distribution (Fig. 1, bottom), the angular diameter distance ratio histogram is heavily skewed towards $DA_{\text{abs}}/DA_{\text{QSO}} = 1$, where a large number of the searches for intervening 21-cm absorption have recently occurred (Gupta et al. 2009; Kanekar et al. 2009b). It is also evident that above angular diameter distance ratios of $DA_{\text{abs}}/DA_{\text{QSO}} =$

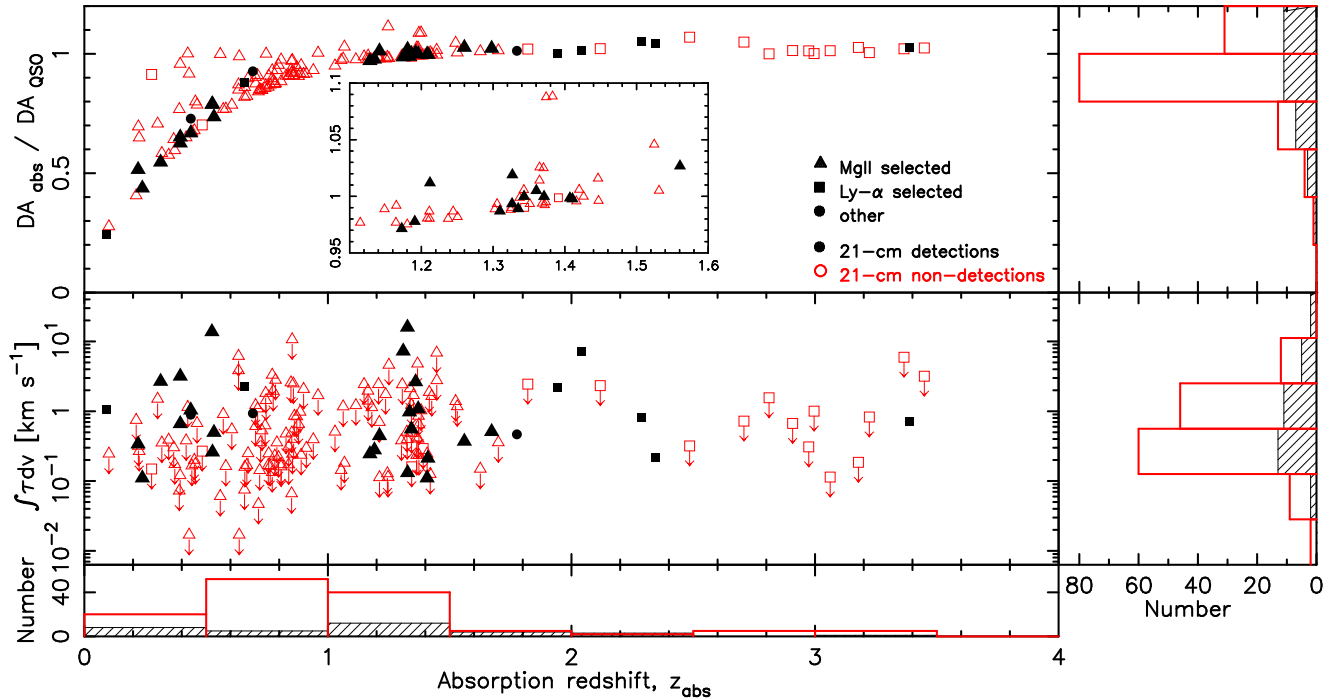


Figure 1. Top: The absorber/quasar angular diameter distance ratio versus the absorption redshift. Note the mix of $DA_{\text{abs}}/DA_{\text{QSO}}$ ratios at $z_{\text{abs}} \lesssim 1$, whereas at $z_{\text{abs}} \gtrsim 1$ the ratio is always large. The filled symbols/hatched histogram represent the 21-cm detections and the unfilled symbols/histogram the non-detections, with the shapes designating the transition through which the absorber was discovered. The inset shows the detail around the $z_{\text{abs}} = 1.1 - 1.6$ region. Bottom: The velocity integrated optical depths versus the absorption redshift, where the arrows designate upper limits (for these the line-widths have been estimated from $W_r^{\lambda 2796}$, see Sect. 2.3.2). In both plots we show the DLAs plus all of the Mg II absorption ($W_r^{\lambda 2796} > 0 \text{ \AA}$) systems searched in 21-cm.

0.8, that the ratio of detections to non-detections drops drastically (shown by the upper two histogram bars in Fig. 1, top)¹.

This, however, is based on a relatively small sample at $DA_{\text{DLA}}/DA_{\text{QSO}} \leq 0.8$ and so we refer to the binomial probabilities of such a distribution occurring by chance: Assuming that there is an equal probability of either a detection or a non-detection occurring in either $DA_{\text{abs}}/DA_{\text{QSO}}$ bin, we see that at $DA_{\text{abs}}/DA_{\text{QSO}} < 0.8$ there is a near certainty of obtaining the observed number detections of detections, $P(\geq k/n) > 0.9$ (Table 2). However, in the $DA_{\text{abs}}/DA_{\text{QSO}} \geq 0.8$ bin, the probability of the observed number of non-detections or more occurring by chance is very small, $P(\geq k/n) \lesssim 10^{-15}$.

For the $W_r^{\lambda 2796} > 0.6 \text{ \AA}$ Mg II absorbers with $1 < W_r^{\lambda 2796}/W_r^{\lambda 2600} < 2$ AND $W_r^{\lambda 2852} > 0.1 \text{ \AA}$, i.e. those in which $\approx 40\%$ are known to be DLAs (Rao et al. 2006), we obtain a similar distribution at $DA_{\text{abs}}/DA_{\text{QSO}} \geq 0.8$, although the probabilities are much higher (row 3 of Table 2), due to the smaller sample. However, a probability of $P(\geq k/n) = 1.36 \times 10^{-4}$ is still significant at 3.81σ , assuming Gaussian statistics, compared with $P(\geq k/n) = 0.026 \Rightarrow 2.23\sigma$ for the confirmed DLAs only (Curran & Webb 2006), where there were 16 non-detections out of a sample of 22 at $DA_{\text{abs}}/DA_{\text{QSO}} \geq 0.8^2$.

From the bottom panel of Fig. 1, it is apparent that the 21-cm

surveys cover a wide range of sensitivities and with no knowledge of the total neutral hydrogen column densities in many of these, it is not possible to normalise out the observational biases (Sect. 2.1). However, the histogram in Fig. 1 shows that, on the whole, the non-detections have been searched as deeply as the detections and, given that the observed distribution may be driven by other effects³, all else being equal, the angular diameter distance ratio does appear to be correlated with the detection rate.

To recap, for all of the Mg II absorption systems the observed detection rate at low angular diameter distance ratios has a high probability of occurring by chance, while that at high ratios is extremely unlikely and, when placing conditions on the sample, by selecting those which could be DLAs, there is an extremely high detection rate at low angular diameter distance ratios, while the rate remains low at high ratios. Since, on the basis that a given absorption cross-section will cover a given emission region less effectively when these are at similar angular diameter distances, it stands to reason that the observed distribution is, at least in part, driven by the line-of-sight geometry.

2.3 Mg II equivalent width

2.3.1 21-cm line width

While the above work demonstrates that the detection rate appears to be dependent upon the angular diameter distance ratio, the

¹ The choice of a cut at $DA_{\text{abs}}/DA_{\text{QSO}} = 0.8$ is somewhat arbitrary, but, as Curran & Webb (2006), we use this value since it is the lowest which gives an appreciable enough sample size in the lower bin.

² Combined with the $\geq 11/13$ detections at $DA_{\text{abs}}/DA_{\text{QSO}} < 0.8$, this gives an overall probability of $0.00029 (\Rightarrow 3.63\sigma)$ for the whole distribution.

³ Such as different T_{spin}/f ratios (see Curran et al. 2007c) or column densities (see Sect. 3).

Table 2. The statistics of the whole sample [Fig. 1], that of the absorbers with $W_r^{\lambda 2796} \geq 1.0 \text{ \AA}$, those likely to be DLAs according to Rao et al. (2006), as well as those likely to be DLAs by our definition [Sect. 2.3.1]. We show the number of detections/total with angular diameter distance ratios of $DA_{\text{abs}}/DA_{\text{QSO}} < 0.8$ and the number of non-detections/total with $DA_{\text{abs}}/DA_{\text{QSO}} \geq 0.8$ with the binomial probability of this number or more of occurring by chance. “rate” gives the detection rate for each $DA_{\text{abs}}/DA_{\text{QSO}}$ bin.

Sample	Lyman- α and Mg II						Mg II only					
	DETECTIONS		rate	NON-DETECTIONS		rate	DETECTIONS		rate	NON-DETECTIONS		rate
	< 0.8	$P(\geq k/n)$		≥ 0.8	$P(\geq k/n)$		< 0.8	$P(\geq k/n)$		≥ 0.8	$P(\geq k/n)$	
Whole	11/29	0.93	38%	111/133	8.55×10^{-16}	17%	9/26	0.96	35%	95/109	2.88×10^{-16}	13%
$W_r^{\lambda 2796} \geq 1.0 \text{ \AA}$	11/14	0.029	79%	88/106	1.49×10^{-12}	17%	9/11	0.033	82%	72/82	5.11×10^{-13}	12%
Rao et al. (2006)	8/9	0.020	89%	44/60	1.97×10^{-4}	27%	7/7	0.0078	100%	33/42	1.36×10^{-4}	21%
$W_r^{\lambda 2852} > 0.5 \text{ \AA}$	9/10	0.011	90%	44/64	0.0020	31%	7/7	0.0078	100%	33/46	0.0023	28%

strength of the 21-cm absorption (normalised by the neutral hydrogen column density, $\int \tau dv / N_{\text{HI}}$) may itself be related to the Mg II equivalent width, as shown to apply to the confirmed DLAs (Curran et al. 2007c). However, no such correlation was found between τ and $W_r^{\lambda 2796}$, with only a weak trend existing between $\int \tau dv$ and $W_r^{\lambda 2796}$. The correlation therefore appears to be dominated by the velocity spread of the 21-cm profile (both FWHM and total velocity spread), “significant” at 1.80σ , which rises to 2.30σ when the outlier 1622+238 is removed⁴: With a FWHM = 235 km s^{-1} and an impact parameter of ≈ 75 kpc (Curran et al. 2007b and references therein), this is a most unusual DLA in which we believe the 21-cm profile width is dominated by large-scale dynamics.

Gupta et al. (2009); Kanekar et al. (2009b) report no correlation between the FWHM and $W_r^{\lambda 2796}$ for the Mg II absorbers and in Fig. 2 we show the confirmed DLAs (where $N_{\text{HI}} \geq 2 \times 10^{20} \text{ cm}^{-2}$) together with various sub-sets of Mg II absorbers detected in 21-cm and do find that the addition of the Mg II absorbers degrades the correlation (top panel). This regains a similar significance to that of the DLAs only (Curran et al. 2007c) when only the Mg II absorbers with $W_r^{\lambda 2796} > 1 \text{ \AA}$ are added (second panel) and degrades once more with the condition of Rao et al. (2006) applied to the Mg II absorbers which overlap the same $W_r^{\lambda 2796} / W_r^{\lambda 2600} - W_r^{\lambda 2852}$ space as the confirmed DLAs (third panel).

Through various trials, we only find a significant increase in the correlation for the Mg II absorbers with $W_r^{\lambda 2852} > 0.5 \text{ \AA}$ added to the confirmed DLAs (bottom panel). Although found empirically, our condition actually selects a sub-set of the range specified by Rao et al. (2006), where $\approx 40\%$ of the Mg II absorbers are DLAs. At $W_r^{\lambda 2852} > 0.5 \text{ \AA}$, 16 of the 30 absorbers are DLAs (50%), cf. 16 out of 49 (30%) at $1 < W_r^{\lambda 2796} / W_r^{\lambda 2600} < 2$ AND $0.1 < W_r^{\lambda 2852} < 0.5 \text{ \AA}$ (figure 11 of Rao et al. 2006). Above $W_r^{\lambda 2852} \approx 1 \text{ \AA}$, all of the Mg II absorbers are DLAs, although being a sample of only four severely restricts the significance of this⁵.

Note that, although our $W_r^{\lambda 2852} > 0.5 \text{ \AA}$ selection is a sub-set of the DLA range of Rao et al. (2006), our FWHM- $W_r^{\lambda 2796}$ correlation is significantly higher than when applying their con-

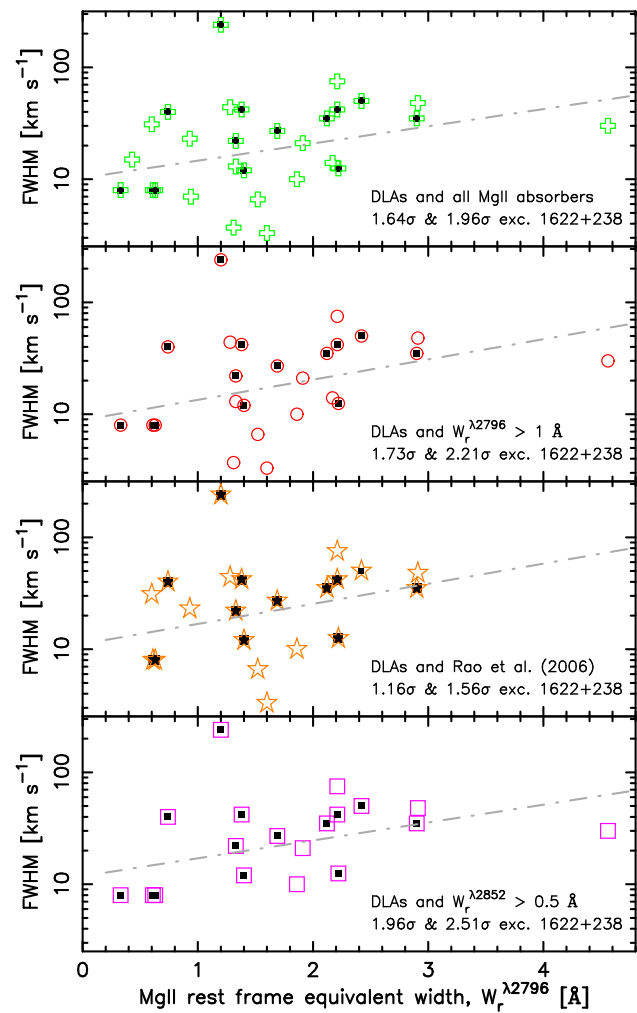


Figure 2. The full width half maximum of the 21-cm absorption profile versus the Mg II 2796 Å equivalent width for the DLAs and Mg II absorption systems. All of the panels show the confirmed DLAs (small black squares) overlain with the unfilled symbols, which show various Mg II absorber sub-samples – all Mg II absorbers detected in 21-cm, those with 2796 Å equivalent widths of $W_r^{\lambda 2796} > 1 \text{ \AA}$, those which could be DLAs according to Rao et al. (2006) [$1 < W_r^{\lambda 2796} / W_r^{\lambda 2600} < 2$ AND $W_r^{\lambda 2852} > 0.1 \text{ \AA}$, where $0.6 \leq W_r^{\lambda 2796} < 3.3 \text{ \AA}$] and finally those with just $W_r^{\lambda 2852} > 0.5 \text{ \AA}$. In each panel we give the significance of the correlation for the DLAs plus Mg II absorbers with and without the outlier 1622+238, with the line showing the least-squares fit to the latter.

⁴ Curran et al. (2007c) previously reported a significance of 2.21σ (2.84σ without 1622+238) for the FWHM- $W_r^{\lambda 2796}$ correlation, but here we exclude 0248+430 (at $W_r^{\lambda 2796} = 1.86 \text{ \AA}$, FWHM = 19 km s^{-1}) which, while generally being regarded as a DLA, has an unknown neutral hydrogen column density. Also, we have included 2003–025 (Kanekar et al. 2009b), which at $W_r^{\lambda 2796} = 0.74 \text{ \AA}$, FWHM = 40 km s^{-1} , is somewhat of an outlier.

⁵ For example, applying this condition to the 21-cm absorbers gives only three Mg II systems in addition to the DLAs (cf. the already low number of five when applying $W_r^{\lambda 2852} > 0.5 \text{ \AA}$, Fig. 2). These three do increase the significance of the correlation slightly to 1.82σ (2.36σ without 1622+238).

dition. This can be attributed to the inclusion of the end point at $W_r^{\lambda 2796} = 4.56 \text{ \AA}$ and $\text{FWHM} = 30 \text{ km s}^{-1}$ (towards J0850+5159, Gupta et al. 2009)⁶, as well as a tighter selection which introduces some differences in the sample at $W_r^{\lambda 2796} \lesssim 2 \text{ \AA}$ (the third cf. the bottom panel of Fig. 2).

2.3.2 21-cm line strength

Although the normalised 21-cm line strength may be correlated with the Mg II 2796 Å equivalent width for the confirmed DLAs, Curran & Webb (2006) noted that the 21-cm non-detections span a similar range of equivalent widths. Therefore, while $W_r^{\lambda 2796}$ may be a diagnostic of the 21-cm line strength ($\int \tau dv / N_{\text{HI}} \propto f / T_{\text{spin}}$), it cannot predict whether or not 21-cm will be detected. One possible explanation is that the non-detections are disadvantaged through geometry effects, as discussed in Sect. 2.2.

In Fig. 3 we show the line strength against the equivalent width together with the angular diameter distance ratios. From this, we see that the non-detections are indeed disadvantaged, with most of these being at angular diameter distance ratios of $\gtrsim 0.9$, whereas the detections have a range of ratios, with the large spiral galaxies located at the high end with the strongest line strengths (see figure 6 of Curran et al. 2007c). This is strong evidence that the geometry is, once again, a dominant effect, although applying a survival analysis to the non-detections⁷, raises the significance of the correlation of the whole sample quite dramatically: 2.52σ (2.97σ without 1622+238), cf. 1.59σ (2.07σ without 1622+238)⁸ for the detections only (Curran et al. 2007c). Hence, if the 21-cm line strength and Mg II equivalent width are related, this suggests that many of the non-detections may only require slightly deeper searches.

The values used to derive the limits for the 21-cm non-detections (Fig. 3) will of course be biased by the use of the correlation for the detections to estimate the FWHM of the non-detections. This gives $\text{FWHM} \approx 13 W_r^{\lambda 2796}$ (figure 6 of Curran et al. 2007c), and, where the Mg II equivalent widths are not available (generally at $z_{\text{abs}} \gtrsim 2.2$), we estimate these from the metallicity via $W_r^{\lambda 2796} \approx 2.0 [\text{M}/\text{H}] + 4.0$ (figure 7 of Curran et al. 2007c). When none are available, we apply the average 20 km s^{-1} of the DLAs detected in 21-cm absorption (Curran et al. 2005). Here, the 21-cm detections span a FWHM of 8 to 50 km s^{-1} (or 235 km s^{-1} including 1622+238), giving an average value of 26 km s^{-1} and applying the methods above gives 5 to 28 km s^{-1} for the non-detections, with an average value of 15 km s^{-1} . If instead we just assume the average value of the detections as the FWHM of each non-detection, each of these moves these further up the ordinate in Fig. 3, while reducing the significance of the correlation to 2.07σ (2.56σ without 1622+238).

The fact that, for the DLAs, the normalised line strength exhibits the strongest correlation with equivalent width (followed by the FWHM then $\int \tau dv$, Curran et al. 2007c), suggests that these parameters are inseparable, giving $W_r^{\lambda 2796} \propto f / T_{\text{spin}}$, where f is generally lower for the non-detections as a result of the higher angular diameter distance ratios. In the absence of measured neutral hydrogen column densities, this means that we cannot use the majority of the Mg II absorbers to verify this. Conversely, the corre-

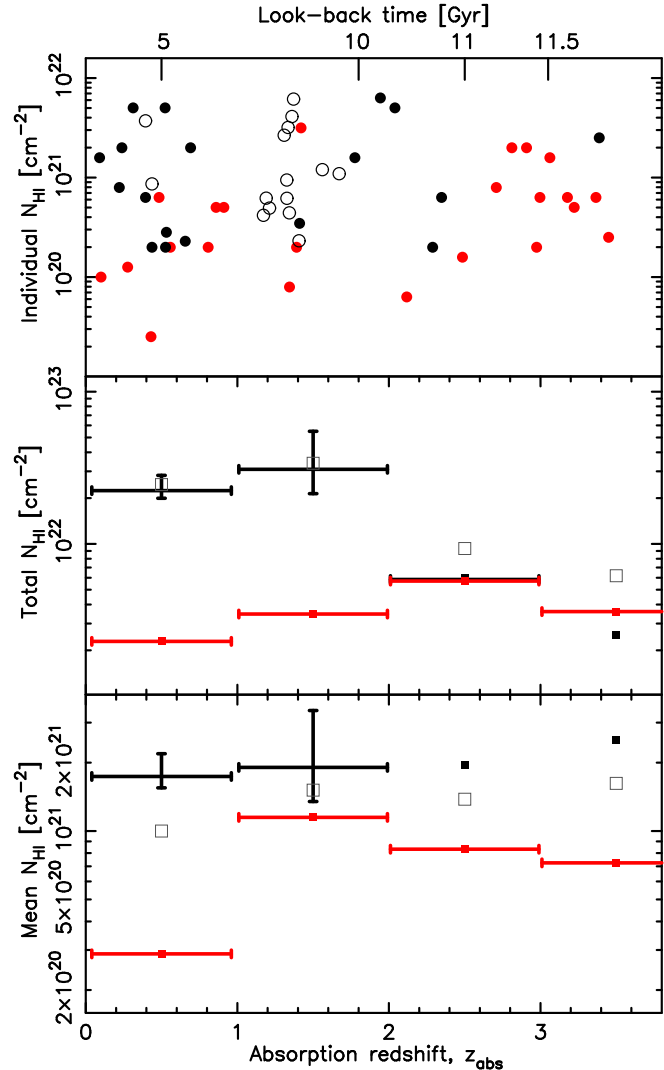


Figure 4. The column density–redshift distribution of the Mg II absorbers searched for in 21-cm, where the black markers denote the detections and the coloured markers the non-detections. Top: The individual column densities, where the filled markers show the actual column density measurements and the unfilled markers show the column density calculated from the 21-cm line strength as per the fit in Fig. 3. We do not include the limits determined from the 21-cm non-detections for which there are no measurements of N_{HI} . Middle: The total values in $\Delta z = 1$ redshift bins. Bottom: The mean N_{HI} per absorber within each bin. The error bars on the ordinate show the 1σ uncertainty to the fit in Fig. 3 and the unfilled squares show the detected and non-detected values combined.

lation may provide a method with which to estimate these column densities, one use of which we now explore.

3 REDSHIFT DISTRIBUTION OF THE NEUTRAL GAS

Using the fit from the 21-cm line strength–Mg II 2796 Å equivalent width correlation (Fig. 3), we can estimate total neutral hydrogen column densities for the Mg II absorbers for which these are unavailable, which we show in Fig. 4. What is immediately clear is that the 21-cm non-detections have systematically lower column densities than the absorbers detected in 21-cm, particularly at low redshift ($0 < z_{\text{abs}} < 1$, where many do have a measured

⁶ Excluded in the $0.6 \leq W_r^{\lambda 2796} < 3.3 \text{ \AA}$ Rao et al. (2006) sample.

⁷ Via the ASURV package (Isobe et al. 1986).

⁸ Updated from Curran et al. (2007c), as per the changes described in footnote 4.

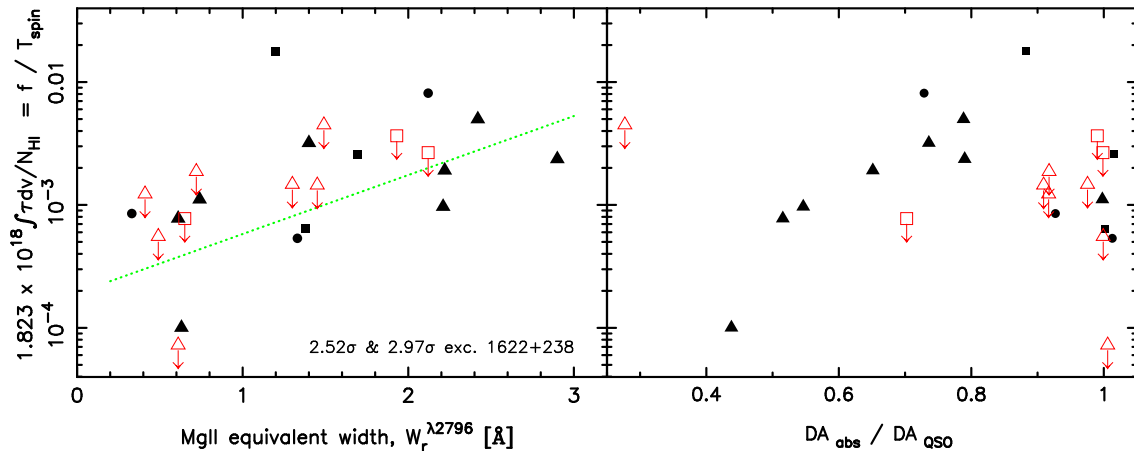


Figure 3. The 21-cm line strength versus the rest frame equivalent width of the Mg II 2796 Å line (left) and the angular diameter distance ratio (right) for the DLAs searched in 21-absorption. The line in the left panel shows the least-squares fit to all of the points. The symbols are as per Fig. 1.

N_{HI})⁹. Although there is considerable overlap in the column densities between the detections and the non-detections, the lower values combined with the geometry issues addressed above, could account for the paucity of strong 21-cm absorption in these objects. Curran et al. (2005) previously noted a correlation between the velocity integrated optical depth and the column density for the confirmed DLAs, which is found to be significant at 3.08σ when the non-detections are also included (Curran et al. 2009).

In the middle panel of Fig. 4 we show the total column density for all of the 21-cm searched absorbers, which have a measured/estimated value of this. It is apparent that, after a possible peak in the $1 < z_{\text{abs}} < 2$ bin, N_{HI} decreases with redshift. However, this will be heavily influenced by the relative paucity of high redshift searches, due to the availability of specific radio bands in conjunction with a severe radio interference environment, which can hamper searches at these frequencies. This effect, in addition to the geometry effects discussed above, could explain the steep decrease in the number of 21-cm absorbers with redshift (Gupta et al. 2009), which runs contrary to the increase in the number of DLAs (Rao et al. 2006).

Therefore in the bottom panel we show the mean column density per bin which, although limited by the very few points in the high redshift bins, shows no evidence of an evolution of N_{HI} . Using these combined averages ($\overline{N_{\text{HI}}}$), we may calculate the cosmological mass density of the neutral gas in the Universe as a function of redshift, via:

$$\Omega_{\text{neutral gas}} = \frac{\mu m_{\text{H}} H_0}{c \rho_{\text{crit}}} n_{\text{DLA}} \overline{N_{\text{HI}}} \frac{1}{(z+1)^2} \frac{H_z}{H_0},$$

where $\mu = 1.3$ is a correction for the 75% hydrogen composition, m_{H} is the mass of the hydrogen atom, $H_0 = 71 \text{ km s}^{-1}$ is the present Hubble parameter, c the speed of light, $\rho_{\text{crit}} \equiv 3 H_0^2 / 8 \pi G$ is the critical mass density of the Universe¹⁰ and

$$\frac{H_z}{H_0} = \sqrt{\Omega_{\text{matter}} (z+1)^3 + (1 - \Omega_{\text{matter}} - \Omega_{\Lambda}) (z+1)^2 + \Omega_{\Lambda}},$$

where H_z is the Hubble parameter at redshift z and we use

⁹ Although the column density is normalised out in Fig. 3, suggesting that, apart from the angular diameter distance ratios, these have been searched sufficiently deeply.

¹⁰ Where G is the gravitational constant.

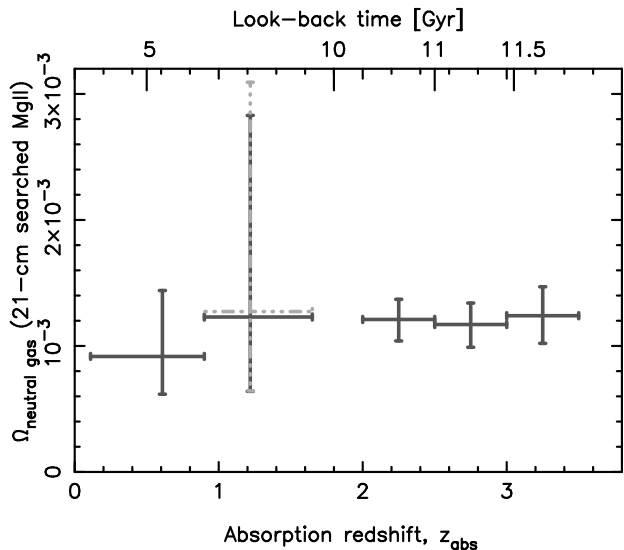


Figure 5. The cosmological mass density versus redshift for the Mg II absorbers searched for in 21-cm. The error bars show the combined uncertainties from $\overline{N_{\text{HI}}}$ (above) and n_{DLA} in each redshift bin (Prochaska & Herbert-Fort 2004; Rao et al. 2006). The dashed-dotted bars in the $0.90 < z_{\text{abs}} \leq 1.65$ bin show the result if the $W_r^{\lambda 2796} > 0.5 \text{ \AA}$ condition of Kanekar et al. (2009b) is applied.

$\Omega_{\text{matter}} = 0.27$ and $\Omega_{\Lambda} = 0.73$. From the redshift number density of DLAs, n_{DLA} (Prochaska & Herbert-Fort 2004; Rao et al. 2006) and deriving the mean column densities according to how the n_{DLA} values are binned in redshift, we obtain the cosmological mass density distribution shown in Fig. 5.

From this we see a near constant $\Omega_{\text{neutral gas}} \approx 1 \times 10^{-3}$, as previously noted by Rao & Turnshek (2000); Prochaska & Herbert-Fort (2004); Rao et al. (2006), where the cosmological mass density of the neutral gas remains unchanged up to redshifts of $z_{\text{abs}} \approx 4$. This is not surprising as our Mg II/DLA sample¹¹ is comprised of sub-sets of the aforementioned samples.

¹¹ Note that while all of the sample is not necessarily comprised of DLAs, from Fig. 4 it is apparent that at least all of the 21-cm detections have $N_{\text{HI}} \geq 2 \times 10^{20} \text{ cm}^{-2}$, including the column densities estimated from the 21-cm detections (unfilled markers). Although some of the 21-cm non-

The fact that our value at $1.1 \lesssim z_{\text{abs}} \lesssim 1.6$ is consistent with that of Rao et al. (2006), provides a check on 21-cm line strength–Mg II 2796 Å equivalent width correlation (Fig. 3). However, it is nearly double the value of $\Omega_{\text{neutral gas}}$ calculated at this redshift by Kanekar et al. (2009b)¹², although this work assumes an average HI column density at these redshifts, whereas our value is estimated using the correlation.

4 DISCUSSION AND SUMMARY

Following the recent surveys of Mg II absorbers at $0.58 < z_{\text{abs}} < 1.70$ (Gupta et al. 2009; Kanekar et al. 2009b), there has been a large increase in the number of intervening 21-cm absorption systems detected at these redshifts. Both these works discuss various reasons regarding the detection of 21-cm absorption in Mg II systems, but these focus upon the various equivalent widths of the singly ionised and neutral metal lines, without considering the possible line-of-sight geometry effects, although these have been found to bias the detection rate for confirmed damped Lyman- α absorption systems (Curran & Webb 2006). Considering this effect, we find for the Mg II absorbers:

- (i) For the sample as a whole (or limiting this to strong Mg II absorbers, e.g. $W_r^{\lambda 2796} > 1 \text{ \AA}$), the mix of detections at low redshifts is what would be expected purely from chance, although the high non-detection rate at $z_{\text{abs}} \gtrsim 1$ is highly unlikely.
- (ii) When restrictions are applied to the sample, so that a large fraction of the Mg II absorbers are expected to consist of DLAs (according to Rao et al. 2006), detection rates of $\approx 100\%$ are reached at low redshift, while the low detection probabilities at $z_{\text{abs}} \gtrsim 1$ remain significant.

Although other factors may contribute (such as lower column densities for the 21-cm non-detections, Sect. 3), which may be unmeasurable (i.e. T_{spin}/f in the absence of N_{HI}), it is apparent that the likelihood of detecting 21-cm absorption is correlated with the angular diameter distance ratio for all intervening absorption systems, where the absorbers at low redshift are subject to a range of $DA_{\text{abs}}/DA_{\text{QSO}}$ ratios and thus exhibit a mix of detections and non-detections, whereas those at $z_{\text{abs}} \gtrsim 1$ all have $DA_{\text{abs}}/DA_{\text{QSO}} \sim 1$, while tending to be non-detections.

Since a given absorber will occult the background flux much more effectively at a lower angular diameter distance ratio, this suggests a strong contribution by the covering factor, which is independent from the measured 21-cm line strength, from which the spin temperature/covering factor degeneracy cannot be broken (Sect. 2.1): In some cases the covering factor has been estimated as the ratio of the compact unresolved component’s flux to the total radio flux (Briggs & Wolfe 1983; Kanekar et al. 2009a). However, even if high resolution radio images at the redshifted 21-cm frequencies are available, this method gives no information on the extent of the absorber (or how well it covers the emission). Furthermore, the high angular resolution images are of the continuum only and so do not give any information about the depth of the line when the extended continuum emission is resolved out. By using the angular diameter distance ratios, we completely circumvent these issues, although we can only discuss generalities which cannot determine values of T_{spin} or f for individual systems. What we

do find, however, from our statistically large sample (a total of 162 absorption systems), is that 21-cm detection rates are much lower when the absorber and background QSO are at similar angular diameter distances.

Saying this, the recent surveys (Gupta et al. 2009; Kanekar et al. 2009b) yield 13 new detections between them at $z_{\text{abs}} \sim 1$, where the angular diameter distance ratios are high ($DA_{\text{abs}}/DA_{\text{QSO}} \gtrsim 0.8$, Fig. 1). However, each of these surveys also yields a large number of non-detections, with both exhibiting a 25% detection rate¹³. This is about double the rate for the whole $DA_{\text{DLA}}/DA_{\text{QSO}} > 0.8$ sample, but very close to that when restrictions are applied to include those Mg II absorbers which may also be DLAs (Table 2). This is not surprising since the Kanekar et al. (2009b) survey selects only those with $W_r^{\lambda 2796} > 0.5 \text{ \AA}$ (the minimum equivalent width of a DLA in the Rao et al. 2006 sample – see their figure 2) and Gupta et al. (2009) select those with $W_r^{\lambda 2796} > 1 \text{ \AA}$, restricting this further.

Another possible factor affecting the detection of 21-cm absorption could be the correlation between the 21-cm line strength ($\int \tau dv/N_{\text{HI}} \propto f/T_{\text{spin}}$) and the Mg II 2796 Å equivalent width ($W_r^{\lambda 2796}$, Curran & Webb 2006). However, the same range of equivalent widths is also spanned by the non-detections, making this a questionable diagnostic with which to find 21-cm absorption systems. We do find, however, that eight of the ten non-detections have $DA_{\text{abs}}/DA_{\text{QSO}} > 0.9$, whereas the 13 detections are much more spread out, spanning $0.4 < DA_{\text{abs}}/DA_{\text{QSO}} < 1$, which suggests that geometry effects may again be responsible for the detection rate. If the $\int \tau dv/N_{\text{HI}} \propto f/T_{\text{spin}} - W_r^{\lambda 2796}$ correlation holds up, the fact that the non-detections increase the significance, suggests that these absorbers may be close to 21-cm detection. In any case, we suggest that $W_r^{\lambda 2796}$ in conjunction with the value of $DA_{\text{abs}}/DA_{\text{QSO}}$ may provide a diagnostic with which to find 21-cm absorption.

As discussed by Curran et al. (2007c), the strongest contributor to this correlation appears to be the 21-cm profile width, which is not surprising as at $W_r^{\lambda 2796} \gtrsim 0.3 \text{ \AA}$, the range discussed here, the Mg II profile is dominated by velocity structure (Ellison 2006). Including all of the Mg II absorbers degrades the correlation (as found by Gupta et al. 2009; Kanekar et al. 2009b), although through the testing of many different equivalent widths and their ratios (e.g. $W_r^{\lambda 2796}$, $W_r^{\lambda 2852}$ & $W_r^{\lambda 2796}/W_r^{\lambda 2600}$), we find that the correlation increases for the Mg II absorbers for which the Mg I 2852 Å equivalent width is $W_r^{\lambda 2852} > 0.5 \text{ \AA}$. At 13.60 eV, HI has a similar ionisation potential to the singly ionised metal species (15.04 for Mg II & 16.18 eV for Fe II), although it is not surprising that the cooler component (i.e. the 21-cm) is better traced by the neutral metal species (i.e. Mg I, which has a potential of 7.65 eV). Furthermore, the fact that $W_r^{\lambda 2852} > 0.5 \text{ \AA}$ is a sub-set of the $W_r^{\lambda 2796}/W_r^{\lambda 2600} - W_r^{\lambda 2852}$ space which contains all of the DLAs of Rao et al. (2006), suggests that the $W_r^{\lambda 2852} > 0.5 \text{ \AA}$ selection is (mostly) adding further DLAs to the confirmed DLA sample (Curran et al. 2007c). That is, in general, the 21-cm profile width is correlated with $W_r^{\lambda 2796}$ when $N_{\text{HI}} \geq 2 \times 10^{20} \text{ cm}^{-2}$.

Investigating this further, in Fig. 6 we show the total neutral hydrogen column density versus the Mg I 2852 Å equivalent width for the $z_{\text{abs}} < 1.7$ absorbers for which both measurements are available. Although there is no clear partitioning, all (in an admit-

detections have $N_{\text{HI}} \lesssim 10^{20} \text{ cm}^{-2}$, from the bottom panel of Fig. 4 the mean value exceeds the defining DLA column density in all redshift bins.

¹² Even when applying their $W_r^{\lambda 2796} > 0.5 \text{ \AA}$ criterion (Fig. 5).

¹³ The binomial probability of 26 or more non-detections out of a sample of 35 is $P(\geq k/n) = 0.0030$ (Gupta et al. 2009, where at $1.10 < z_{\text{abs}} < 1.45$ all of the systems have $DA_{\text{abs}}/DA_{\text{QSO}} \sim 1$).

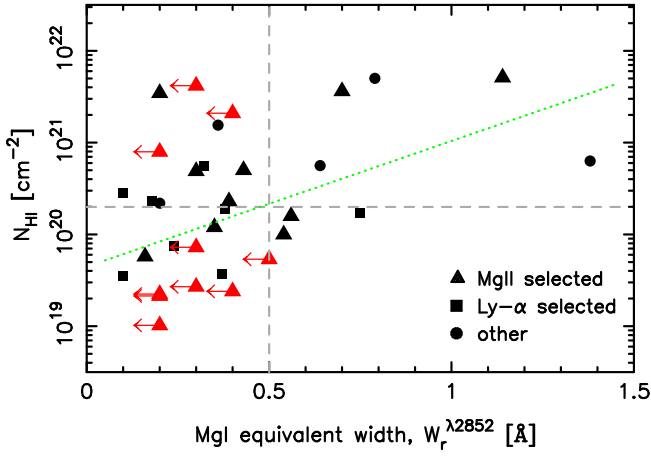


Figure 6. The total neutral hydrogen column density versus the Mg I 2852 Å equivalent width for $z_{\text{abs}} < 1.7$ absorbers (Péroux et al. 2004). The coloured symbols/arrows designate upper limits to $W_r^{\lambda 2852}$. The horizontal dashed line shows $N_{\text{HI}} = 2 \times 10^{20} \text{ cm}^{-2}$, above which the absorbers are considered to be DLAs and the dotted line shows the least-squares fit to all of the points (taking account of the limits via ASURV).

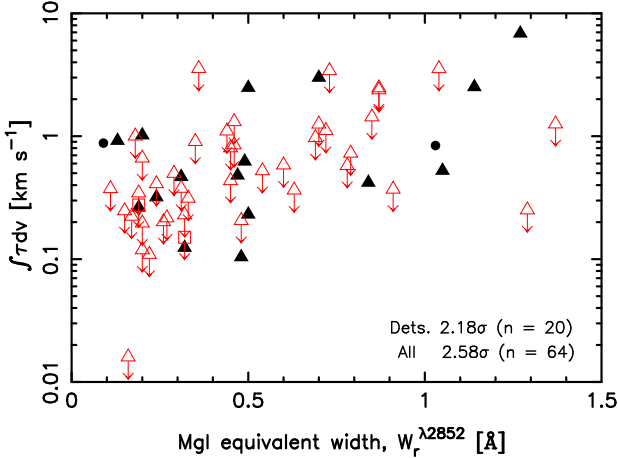


Figure 7. As the left panel of Fig. 3, but with the velocity integrated optical depth of the 21-cm line on the ordinate and the equivalent width of the Mg I 2852 Å line on the abscissa. Note that for $W_r^{\lambda 2852} > 0.5 \text{ Å}$, all of the 21-cm non-detections have $DA_{\text{abs}}/DA_{\text{QSO}} \geq 0.85$.

tedly small sample) of those with $W_r^{\lambda 2852} > 0.5 \text{ Å}$ have $N_{\text{HI}} \gtrsim 10^{20} \text{ cm}^{-2}$, and unlike Péroux et al. (2004), who find no significant correlation between metal line equivalent widths ($W_r^{\lambda 2796}$ & $W_r^{\lambda 2600}$) and N_{HI} , we find $W_r^{\lambda 2852}$ to correlate with $\log_{10} N_{\text{HI}}$ at a 2.83σ significance.

In Fig. 7 we extend this to the sample searched for 21-cm absorption. Ideally, we would show the normalised line strength ($\int \tau dv / N_{\text{HI}} \propto f / T_{\text{spin}}$, as in Fig. 3), however there are only 12 absorbers with measurements of both (comprising of seven 21-cm detections and five non-detections)¹⁴. From this, we see a weak correlation between $\int \tau dv$ and $W_r^{\lambda 2852}$, although, as was noted in Curran et al. (2007c), the neutral hydrogen column density is required in order to obtain the full picture (and f / T_{spin}). The absence

¹⁴ Although these few points do give a 2.21σ correlation between $\int \tau dv / N_{\text{HI}}$ and $W_r^{\lambda 2852}$.

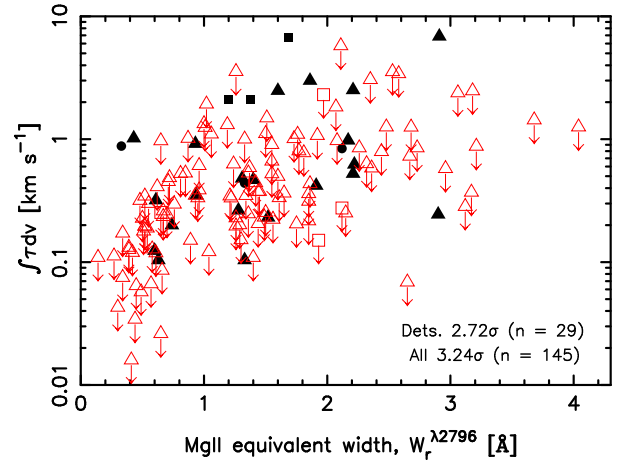


Figure 8. As Fig. 7, but with the equivalent width of the Mg II 2796 Å line on the abscissa.

of a measured N_{HI} could be responsible for the fairly weak correlation, especially considering that the non-detections tend to have lower column densities (Sect. 3).

Finally, for completeness, in Fig. 8 we show $\int \tau dv$ versus the Mg II 2796 Å equivalent width for the whole sample and see that, although the correlation is negligible for the confirmed DLAs only (Curran et al. 2007c), it becomes quite significant over a sample which is an order of magnitude larger. Bear in mind, however, that the FWHMs for the 21-cm non-detections in Fig. 7 and 8 have been estimated from the $\text{FWHM} - W_r^{\lambda 2796} - [\text{M}/\text{H}]$ correlations of the detections (Sect. 2.3.2), which will tend to increase any significance derived for these. This will be tempered somewhat by the optical depth limits for the non-detections, which are known. Therefore the significance of each of these correlations should be considered to lie somewhere between the two quoted values.

To summarise our findings regarding the detectability of 21-cm absorption in intervening Mg II absorption systems:

- On the basis of a 21-cm detection and non-detection being equally probable, at small angular diameter distance ratios ($DA_{\text{abs}}/DA_{\text{QSO}} \lesssim 0.8$) the observed distribution is expected for the whole sample, whereas at high ratios the observed distribution is very improbable. This suggests that the angular diameter distance (DA_{abs}) plays a crucial rôle in the detection of 21-cm absorption, which in turn suggests a strong covering factor dependence.

- Large angular diameter distance ratios may also explain why the non-detections span a similar range of Mg II 2796 Å equivalent widths as the detections, which exhibit a 21-cm line strength– $W_r^{\lambda 2796}$ correlation. Note also, that, in general, the non-detections have considerably lower neutral hydrogen column densities, which could contribute to making these harder to detect over the whole Mg II sample¹⁵.

- Using this correlation to estimate the column densities for the absorbers in which these are unmeasured (particularly at $1.1 \lesssim z_{\text{abs}} \lesssim 1.6$), we find that the cosmological mass density of the neutral gas does not deviate significantly from $\Omega_{\text{neutral gas}} \approx 1 \times 10^{-3}$ over the redshifts spanned by the optically selected absorbers ($0.1 \lesssim z_{\text{abs}} \lesssim 3.5$). This consistency with the general optically

¹⁵ Although N_{HI} is normalised out in our definition of line strength in the case of the $\int \tau dv / N_{\text{HI}} - W_r^{\lambda 2796}$ correlation.

selected population supports the 21-cm line strength– $W_r^{\lambda 2796}$ correlation.

Curran et al. (2007c) suggested that the $\int \tau dv / N_{\text{HI}} - W_r^{\lambda 2796}$ correlation was dominated by the 21-cm profile width in confirmed DLAs, although this does not appear to be the case for the Mg II sample in general (Gupta et al. 2009; Kanekar et al. 2009b). However, we find this significance to increase when only the absorbers with Mg I 2852 Å equivalent widths of $W_r^{\lambda 2852} > 0.5$ Å are added. This happens to be a sub-set of the Mg II absorbers with $1 < W_r^{\lambda 2796} / W_r^{\lambda 2600} < 2$ AND $W_r^{\lambda 2852} > 0.1$ Å, $\approx 40\%$ of which are known to be DLAs (Rao et al. 2006). The FWHM– $W_r^{\lambda 2796}$ correlation does therefore appear to hold for absorbers in which the neutral hydrogen column density exceeds $N_{\text{HI}} \sim 10^{20} \text{ cm}^{-2}$. Finally, we note a (somewhat scattered) correlation between the total neutral hydrogen column density and the equivalent width of the Mg I 2852 Å line, although there appears to be no such relation for the singly ionised metal species (Péroux et al. 2004).

ACKNOWLEDGMENTS

I wish to thank the referee for their helpful comments, which aided in clarifying the manuscript. This research has made use of the NASA/IPAC Extragalactic Database (NED) which is operated by the Jet Propulsion Laboratory, California Institute of Technology, under contract with the National Aeronautics and Space Administration. This research has also made use of NASA's Astrophysics Data System Bibliographic Service and ASURV Rev 1.2 (Lavalley et al. 1992), which implements the methods presented in Isobe et al. (1986).

REFERENCES

- Briggs F. H., Wolfe A. M., 1983, ApJ, 268, 76
 Brown R. L., Mitchell K. J., 1983, ApJ, 264, 87
 Brown R. L., Roberts M. S., 1973, ApJ, 184, L7
 Carilli C. L., Lane W., de Bruyn A. G., Braun R., Miley G. K., 1996, AJ, 111, 1830
 Carilli C. L., Rupen M. P., Yanny B., 1993, ApJ, 412, L59
 Chengalur J. N., de Bruyn A. G., Narasimha D., 1999, A&A, 343, L79
 Chengalur J. N., Kanekar N., 2000, MNRAS, 318, 303
 Curran S. J., Darling J. K., Bolatto A. D., Whiting M. T., Bignell C., Webb J. K., 2007a, MNRAS, 382, L11
 Curran S. J., Kanekar N., Darling J. K., 2004, Science with the Square Kilometer Array, New Astronomy Reviews 48. Elsevier, Amsterdam, pp 1095–1105
 Curran S. J., Murphy M. T., Pihlström Y. M., Webb J. K., Purcell C. R., 2005, MNRAS, 356, 1509
 Curran S. J., Tzanavaris P., Darling J. K., Whiting M. T., Webb J. K., Bignell C., Athreya R., Murphy M. T., 2009, MNRAS, In press (arXiv:0910.3742)
 Curran S. J., Tzanavaris P., Murphy M. T., Webb J. K., Pihlström Y. M., 2007b, MNRAS, 381, L6
 Curran S. J., Tzanavaris P., Pihlström Y. M., Webb J. K., 2007c, MNRAS, 382, 1331
 Curran S. J., Webb J. K., 2006, MNRAS, 371, 356
 Curran S. J., Whiting M. T., Wiklind T., Webb J. K., Murphy M. T., Purcell C. R., 2008, MNRAS, 391, 765
 Darling J., Giovanelli R., Haynes M. P., Bower G. C., Bolatto A. D., 2004, ApJ, 613, L101
 de Bruyn A. G., O'Dea C. P., Baum S. A., 1996, A&A, 305, 450
 Ellison S. L., 2006, MNRAS, 368, 335
 Gupta N., Srianand R., Petitjean P., Noterdaeme P., Saikia D. J., 2009, MNRAS, 398, 201
 Isobe T., Feigelson E., Nelson P., 1986, ApJ, 306, 490
 Kanekar N., Briggs F. H., 2003, A&A, 412, L29
 Kanekar N., Chengalur J. N., 2001, A&A, 369, 42
 Kanekar N., Chengalur J. N., 2003, A&A, 399, 857
 Kanekar N., Chengalur J. N., Subrahmanyam R., Petitjean P., 2001, A&A, 367, 46
 Kanekar N., Lane W. M., Momjian E., Briggs F. H., Chengalur J. N., 2009a, MNRAS, 394, L61
 Kanekar N., Prochaska J. X., Ellison S. L., Chengalur J. N., 2009b, MNRAS, 396, 385
 Kanekar N., Subrahmanyam R., Ellison S. L., Lane W., Chengalur J. N., 2006, MNRAS, 370, L46
 Lane W., Smette A., Briggs F. H., Rao S. M., Turnshek D. A., Meylan G., 1998, AJ, 116, 26
 Lane W. M., 2000, PhD thesis, University of Groningen
 Lane W. M., Briggs F. H., 2001, ApJ, 561, L27
 Lane W. M., Briggs F. H., Smette A., 2000, ApJ, 532, 146
 Lavalley M. P., Isobe T., Feigelson E. D., 1992, in BAAS Vol. 24, ASURV, Pennsylvania State University. Report for the period Jan 1990 - Feb 1992.. pp 839–840
 Lovell J. E. J., Reynolds J. E., Jauncey D. L., et al, 1996, ApJ, 472, L5
 Péroux C., Deharveng J.-M., Le Brun V., Cristiani S., 2004, MNRAS, 352, 1291
 Pihlström Y. M., Vermeulen R. C., Taylor G. B., Conway J. E., 1999, ApJ, 525, L13
 Prochaska J. X., Herbert-Fort S., 2004, PASP, 116, 622
 Rao S., Turnshek D., Nestor D. B., 2006, ApJ, 636, 610
 Rao S. M., Turnshek D. A., 2000, ApJS, 130, 1
 Roberts M. S., Brown R. L., Brundage W. D., Rots A. H., Haynes M. P., Wolfe A. M., 1976, AJ, 81, 293
 Wolfe A. M., Briggs F. H., Jauncey D. L., 1981, ApJ, 248, 460
 Wolfe A. M., Briggs F. H., Turnshek D. A., Davis M. M., Smith H. E., Cohen R. D., 1985, ApJ, 294, L67
 Wolfe A. M., Davis M. M., 1979, AJ, 84, 699
 York B. A., Kanekar N., Ellison S. L., Pettini M., 2007, MNRAS, 382, L53